Dalton Transactions

ROYAL SOCIETY OF CHEMISTRY

FRONTIER

View Article Online
View Journal | View Issue

Cite this: *Dalton Trans.*, 2024, **53**, 10403

Layered double hydroxide-based electrode materials derived from metal–organic frameworks: synthesis and applications in supercapacitors

Fujuan Luo,[b] Xiaoguang San, *[a] Yisong Wang,[c] Dan Meng*[a] and Kai Tao *[b]

Received 8th May 2024,
Accepted 14th May 2024

DOI: 10.1039/d4dt01344a

rsc.li/dalton

Metal–organic frameworks (MOFs) have emerged as promising electrode materials for supercapacitors (SCs) due to their highly porous structures, tunable chemical compositions, and diverse morphologies. However, their applications are hindered by low conductivity and poor cycling performance. A novel approach for resolving this issue involves the growth of layered double hydroxides (LDHs) using MOFs as efficient templates or precursors for electrode material preparation. This method effectively enhances the stability, electrical conductivity, and mass transport ability of MOFs. The MOF-derived LDH exhibits a well-defined porous micro-/nano-structure, facilitating the dispersion of active sites and preventing the aggregation of LDHs. Firstly, this paper introduces synthesis strategies for converting MOFs into LDHs. Subsequently, recent research progress in MOF-derived LDHs encompassing pristine LDH powders, LDH composites, and LDH-based arrays, along with their applications in SCs, is overviewed. Finally, the challenges associated with MOF-derived LDH electrode materials and potential solutions are discussed.

1 Introduction

In recent years, the depletion of fossil energy sources and the escalation of global environmental pollution have spurred a heightened demand for green, efficient, and sustainable renewable energy sources, notably solar and wind energy. This demand has propelled the advancement of reliable and efficient electrochemical energy conversion and storage technologies.[1,2] Among them, supercapacitors (SCs) have garnered significant attention owing to their attributes of high power density, rapid charging capability, extended lifespan, and cost-effectiveness, rendering them promising power sources for electric vehicles and portable electronics.[3] Nonetheless, the widespread utilization of SCs faces hindrances due to their limited energy density. Consequently, substantial efforts have been directed towards the exploration of novel electrode materials characterized by high capacitance, conductivity, and cycling stability.[4,5] Based on the charge storage mechanism, electrode materials are classified into capacitive, pseudocapacitive and battery-type materials. Compared with capacitive and pseudocapacitive materials, battery-type materials deliver much higher capacity in virtue of their deep surface faradaic reactions.[6,7]

Layered double hydroxides (LDHs) represent a class of polymetallic clay materials with a chemical formula of $[M^{z+}_{1-x}M^{3+}_{x}(OH)_2]^{x+}[X^{n-}]_{x/n}{\cdot}yH_2O$, where the layers of metal cations (M) are interleaved with compensated anions (X) and water molecules.[8] Due to their high redox activity, distinctive interlayer embedding properties, and environmentally friendly characteristics, LDHs have garnered significant attention as battery-type electrode materials for SCs.[9] Nonetheless, the tendency to agglomerate poses a challenge for lamellar LDHs. Furthermore, the limited electron conductivity results in inferior rate capability. To address these shortcomings, various strategies have been proposed, including the construction of novel nanostructures through sacrificial templating methods, the incorporation of other materials, and oriented growth on conductive substrates.[10–12]

Metal–organic frameworks (MOFs) are multifunctional organic–inorganic hybrid materials composed of metal ions and organic ligands.[13] Their adjustable structure, chemical composition, and morphology make MOFs ideal templates or precursors for synthesizing various electrode materials, such as carbon, metal oxide/hydroxide, metal sulfide, *etc.*[14–17] The MOF derivatives retain the intricate nanostructures of MOFs and serve as a versatile platform for producing multiphase-active compounds.[18] Additionally, the organic ligands in MOFs contain abundant heteroatoms (*e.g.*, C and N), which enhance charge-transfer environments and improve the structural stabi-

[a]*College of Chemical Engineering, Shenyang University of Chemical Technology, Shenyang 110142, China. E-mail: mengdan0610@hotmail.com, sanxiaoguang@syuct.edu.cn*
[b]*School of Materials Science & Chemical Engineering, Ningbo University, Ningbo, Zhejiang 315211, China. E-mail: taokai@nbu.edu.cn*
[c]*Taizhou Technician College, Taizhou 318000, China*

lity and chemical activity of the materials.[19] Recently, there has been significant interest in MOF-derived LDHs for electrochemical energy-related applications due to the following advantages: (1) the MOF is used as both a template and a precursor, which will simplify the synthesis of LDHs, since the removal of the template is avoided. (2) LDHs inherit the porous structure of MOFs, facilitating charge transport. (3) Versatile LDHs with desirable compositions and complex structures can be achieved, considering the high tailorability of MOFs.[20,21] Numerous LDH-based electrode materials derived from MOFs, including pristine LDH powders, LDH composites, and LDH-based arrays, have been extensively investigated.[22–24] In this regard, a summary of the recent advances in this field is urgent to inspire more exploration, but it is still rare in the literature.

In this Frontier, we aim to showcase recent advancements in the synthesis of LDH-based electrode materials derived from MOFs, with specific emphasis on their applications in SCs (Scheme 1). We first introduce the popular synthesis strategies for converting MOF templates into LDHs and then summarize the research progress of LDH-based electrode materials synthesized from MOF precursors and their electrochemical performance in SCs (Table 1). Finally, we address the challenges associated with MOF-derived LDH-based electrode materials and explore potential strategies to overcome them.

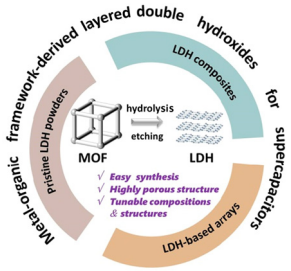

Scheme 1 Schematic illustration of typical MOF-derived LDHs as the electrode materials for SCs.

2 Synthesis strategies for converting MOF templates into LDHs

MOFs have been widely acknowledged as ideal precursors/templates for constructing various electrode materials.[25,26] However, the traditional pyrolysis method not only significantly disrupts the organic ligand skeleton of the MOF template but also entails substantial energy consumption, hindering large-scale production. Therefore, the controllable ionic/ligand exchange method has emerged as the predominant approach for converting MOFs into LDHs.[19] Two commonly employed strategies for the derivation of LDHs from MOFs, namely alkaline hydrolysis and etching, are described below. These strategies are characterized by their mildness and simplicity, resulting in LDHs with tunable compositions, unique nanostructures, and high porosity.

2.1 The hydrolysis strategy

The practical applications of pristine MOFs are significantly hindered by their instability under harsh conditions.[27] In alkaline environments, MOFs undergo hydrolysis. Fortunately,

Table 1 Representative MOF-derived LDH-based electrode materials for SCs

MOF template	Synthesis strategy	Electrode materials	Electrolyte	Electrochemical performance	Ref.
Pristine LDH powders					
NiCo-MOF	Hydrolysis	Ni/Co-LDH-7 : 3	1 M KOH	1652 F g^{-1}@1 A g^{-1}, 100% 2000 cycles	29
NiCo-MOF	Hydrolysis	$Ni_{0.7}Co_{0.3}(OH)_2$	6 M KOH	945 C g^{-1}@0.5 A g^{-1}, 100% 20 000 cycles	30
CoNi-ZIF	Etching	CoNi-LDH4	6 M KOH	1877 F g^{-1}@1 A g^{-1}, 92.1% 5000 cycles	79
Ni-MOF	Etching	NiCo-LDH	3 M KOH	1272 C g^{-1}@2 A g^{-1}, 103.9% 5000 cycles	37
CoMn-MOF	Etching	NiCoMn-LDH	2 M KOH	227.8 mA h g^{-1}@1 A g^{-1}, 85.1% 5000 cycles	40
Co-ZIF-L	Hydrolysis	$Zn_{0.25}Ni_{0.75}Co$-LDH-BA^-	2 M KOH	378 mA h g^{-1}@1 A g^{-1}, 91.2% 10 000 cycles	80
LDH composites					
ZIF-67	Etching	NF/NiCo-LDH/NiMOF/S	1 M KOH	1200 F g^{-1} @1 A g^{-1}, 86% 4000 cycles	81
ZIF-67	Etching	CC@CCH-MOF-LDH HAs	2 M KOH	1700 F g^{-1}@2 A g^{-1}, 91.1% 2500 cycles	82
ZIF-67	Etching	ZIF-67-LDH-CNP-110	6 M KOH	1616 F g^{-1}@1 A g^{-1}, 67.2% 10 000 cycles	83
NiCo-MOF	Hydrolysis	CNTs/NiCo-LDH	2 M KOH	1628 F g^{-1}@1 A g^{-1}, 99.4% 10 000 cycles	51
ZIF-8	Etching	GO/ZnCoNi-LDH	1 M KOH	836.9 C g^{-1}@1 A g^{-1}, 99.0% 10 000 cycles	54
Co-ZIF	Etching	NiCo-LDH@NCF	2 M KOH	756 C g^{-1}@0.5 A g^{-1}, 81.7% 5000 cycles	59
ZIF-67	Etching	NiCoS@PPy	2 M KOH	2316.7 F g^{-1}@1 A g^{-1}, 84% 8500 cycles	60
ZIF-67	Etching	PEDOT@NiCo-LDH/CC	1 M KOH	1508 F g^{-1}@1 A g^{-1}, 90.1% 10 000 cycles	62
ZIF-67	Etching	CoS_x/Ni–Co-LDH	2 M KOH	1562 F g^{-1}@1 A g^{-1}, 76.6% 5000 cycles	65
ZIF-67	Etching	MnO_2@NiCo-LDH/CoS_2	2 M KOH	1547 F g^{-1}@1 A g^{-1}, 81% 2000 cycles	66
ZIF-67	Etching	C/N-NiCoMn-LDH/Ag	2 M KOH	1988 F g^{-1}@1 A g^{-1}, 80.7% 10 000 cycles	70
LDH-based arrays					
ZIF-L	Etching	NiCo-LDH@rGO/NF	1 M KOH	2408.8 F g^{-1}@0.5 A g^{-1}, 80.4% 10 000 cycles	84
ZIF-67	Etching	CuO@NiCo-LDH/CF	2 M KOH	5607 mF cm^{-2}@1 mA cm^{-2}, 93.1% 5000 cycles	74
ZIF-67	Etching	CuO/CF@NiCoMn−OH	6 M KOH	3356 F g^{-1}@1 A g^{-1}, 77.8% 2000 cycles	75
CuCo-ZIF-L	Etching	CuCoNi-OH	3 M KOH	821.6 C g^{-1}@1 A g^{-1}, 82.5% 5700 cycles	76
Co-MOF	Etching	NiCo-LDH/$NiCo_2S_4$/BPQD	6 M KOH	2938.2 F g^{-1}@1 A g^{-1}, 76.5% 10 000 cycles	85
Co-MOF	Etching	NiCo-LDH	6 M KOH	7631 mF cm^{-2}@2 mA cm^{-2}, 70% 10 000 cycles	86

organic ligands can be substituted by OH^- ions, leading to the formation of transition metal hydroxides. Consequently, this strategy can be employed to modify fragile MOFs, thereby enhancing the stability of the materials and optimizing their performance. The LDHs obtained *via* alkaline hydrolysis of MOFs exhibit high redox activity and porosity. However, the uncontrolled growth of LDHs resulting from the rapid collapse of MOFs leads to compromised performance.[28]

To elucidate the hydrolysis mechanism of MOFs under alkaline conditions, Xiao *et al.* conducted a study on the alkaline hydrolysis of MOFs aimed at synthesizing hierarchical microspheres of LDHs through isotopic tracing experiments.[29] Their research revealed that the labeled M_3 (μ_3-^{18}OH) (where M = Ni^{2+} and Co^{2+}) with ^{18}O (as depicted in Fig. 1a) participated in the structural assembly of an LDH, influencing the leaching of metal cations and the growth of hydroxides. Consequently, the optimized LDH inherited the spherical morphology of the MOF template, exhibiting a high surface area and mesoporous channels conducive to rapid charge transport (Fig. 1b and c).

Moreover, another issue arises from the residues in the electrode materials following the hydrolysis of MOFs, which may react with the electrolyte during the charging/discharging process, thus compromising the cycling performance. To address this challenge, Zhang *et al.* investigated a novel strategy aimed at achieving complete hydrolysis of MOF templates by separately heating the MOF and alkaline aqueous solution at high temperatures before mixing (Fig. 1d).[30] This specific hydrolysis strategy facilitated the complete conversion of the MOF, eliminating residues and promoting the tight stacking of hydroxide nanosheets, leading to the formation of a robust core–shell structure (Fig. 1e–h). Consequently, the resulting $Ni_{0.7}Co_{0.3}(OH)_2$ core–shell microspheres exhibited an exceptionally long cycle life.

The hydrolytic transformation represents a relatively mild process that can be easily conducted by adjusting the reaction conditions such as temperature, time, and solution concentration to optimize the electrode materials, ensuring ideal porous structures and morphological features. The self-aggregation of LDHs is mitigated owing to the highly dispersed metal ions within the framework. Additionally, this strategy is economically viable, as the organic ligands replaced by OH^- substitution can be recycled.[31] However, few studies have been conducted using this strategy, primarily because the mechanism of alkaline hydrolysis has not been fully elucidated, hindering precise control over LDH growth. Moreover, this approach is constrained by the challenges associated with synthesizing suitable multimetallic MOF precursors to construct complex LDHs.

2.2 The etching strategy

The etching strategy stands as another common approach for preparing transition metal hydroxides from MOFs, particularly zeolitic imidazolate frameworks (ZIFs). Jiang *et al.* were the first to report the synthesis of three-dimensional (3D) LDH hollow nanopolyhedral structures *via* the etching strategy using ZIF-67 as the template (Fig. 2), and they also elucidated the formation mechanism of LDHs.[32] Firstly, protons were generated from the hydrolysis of metal ions. Subsequently, ZIF-67 underwent gradual etching by protons to release Co^{2+} ions. Concurrently, some Co^{2+} ions were oxidized to Co^{3+} by dissolved O_2 and NO_3^- in the solution. Finally, an LDH was formed through the co-precipitation of metal ions with OH^-. Compared to the hydrolysis strategy of replacing organic ligands with OH^-, the etching strategy offers a more gentle and controllable pathway for LDH formation *via* the co-precipitation process. The morphological features of MOF-derived transition metal hydroxide nanomaterials can be easily tuned by adjusting the etching conditions. Furthermore, during the conversion process, NO_3^- and negatively charged organic ligands can naturally intercalate into the interlayer space of LDHs.[33] Since ZIFs are relatively stable under neutral and alkaline conditions but can easily decompose in acidic solution, they are the most used templates for the etching method. Given the facile synthesis of ZIFs, various types of ZIF composites can be developed as excellent precursors for constructing

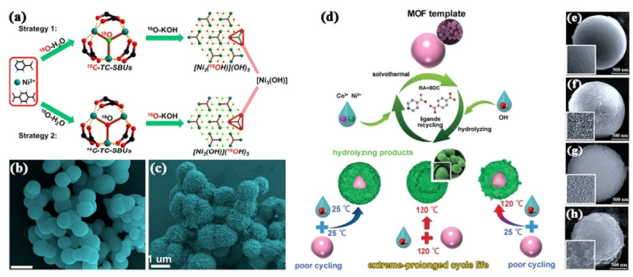

Fig. 1 (a) Isotopic tracing experiments to reveal the hydrolysis mechanism of MOFs. SEM images of the (b) Ni/Co-MOF-7 : 3 precursor and (c) Ni/Co-LDH-7 : 3. Reproduced with permission from ref. 29, Copyright 2019, American Chemical Society. (d) The alkaline hydrolysis of the Ni–Co-MOF through different treatments. SEM images of the (e) MOF template, (f) $Ni_{0.7}Co_{0.3}(OH)_2$-0.1$_M$-SH, (g) $Ni_{0.7}Co_{0.3}(OH)_2$-0.2$_M$-SH and (h) $Ni_{0.7}Co_{0.3}(OH)_2$-0.5$_M$-SH. Reproduced with permission from ref. 30, Copyright 2019, WILEY-VCH.

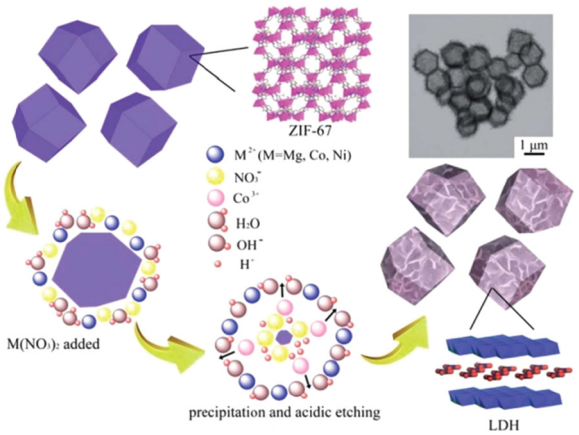

Fig. 2 Illustration showing the formation of LDH nanocages by simultaneous precipitation and acidic etching. Reproduced with permission from ref. 32, Copyright 2013, the Royal Society of Chemistry.

LDH composites with complex structures, offering novel ideas and feasibility for the preparation of high-performance electrode materials. Consequently, the etching strategy is gradually gaining popularity.

3 Various MOF-derived LDHs for supercapacitors

By selecting different metal types (manganese, cobalt, nickel, aluminum, iron, *etc.*), organic linkers (hydroxy acids, imidazoles, *etc.*), and reaction conditions, it is possible to grow various geometrical morphologies of MOF micro-nanostructures *in situ* or on supports. Thus, various MOF-derived LDHs can be designed and explored as electrode materials for SCs.

3.1 Pristine LDH powders

LDHs are promising battery-type electrode materials for SCs, yet their applications are hindered by their inherent low electrical conductivity and tendency to self-stacking.[34,35] Therefore, constructing 3D micro-nanostructures for LDHs has been recognized as an effective strategy to mitigate these drawbacks.[36] Typically, 3D LDHs are fabricated through sacrificial template methods using templates like silica and carbon. However, the tedious and environmentally unfriendly process of removing hard templates poses a challenge. In particular, it is hard to synthesize non-spherical templates. MOFs can serve as both templates and precursors, eliminating the need for template removal and enabling the synthesis of 3D non-spherical LDHs with tunable morphologies. Among LDHs, NiCo-LDHs have garnered significant attention due to their high conductivity, specific capacitance, and stability. Ramachandran *et al.* performed a series of studies on deriving NiCo-LDH from Ni-MOF (organic linker: trimesic acid) microspheres through *in situ* etching.[37] They observed that the hydrolysis and etching time significantly influenced the transformation process of the Ni-MOF, modifying the lamellar and pore structure of NiCo-LDH (Fig. 3a). Notably, large-sized sheets grown on the microspheres (NiCo-LDH/10) generated after 10 hours of etching substantially increased the surface area and pore volume, facilitating rapid ion and electron transport, leading to excellent electrochemical performance, with a maximum specific capacity of 1272 C g^{-1} (Fig. 3b). The prepared asymmetric supercapacitor exhibited a high energy density of 36.1 W h kg^{-1} with impressive cycling durability close to 100% after 5000 cycles (Fig. 3c).

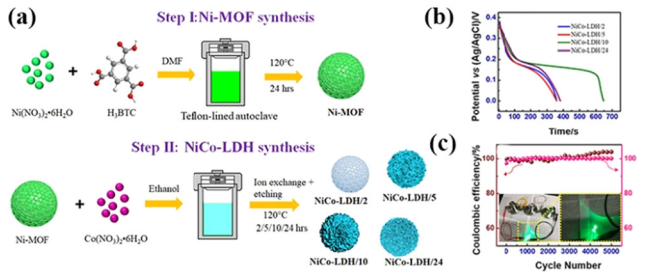

Fig. 3 (a) Schematic diagram of the synthesis of the Ni-MOF template and derived NiCo-LDHs. (b) GCD curves of NiCo-LDH at 1 A g^{-1}. (c) Cycling performance and the coulombic efficiency of NiCo-LDH/10// CNT at 4 A g^{-1}. Reprinted with permission from ref. 37, Copyright 2020, American Chemical Society.

Introducing heterometals (such as Mn, Mo, Ce, *etc.*) into binary LDHs can enhance their electrochemical performance by improving charge transfer and increasing redox active sites. Ternary LDHs, with multiple valences and improved conductivity, exhibit superior capacity and cycling stability compared to binary LDHs. Manganese (Mn) is particularly notable for its high conductivity, rich oxidation states, high theoretical capacity, and abundance, facilitating its wide application in enhancing the electrochemical performance of binary LDHs.[38] We reported the synthesis of Ni–Co–Mn LDH hollow nanocages by etching bimetallic CoMn-ZIF with nickel nitrate. The resulting Ni–Co–Mn LDH exhibited significantly better performance in specific capacitance and rate performance compared to the binary Ni–Co LDH.[39] Similarly, Dai *et al.* prepared NiCoMn-LDH electrode materials by Ni ion etching a bimetallic CoMn-MOF with different Co/Mn ratios.[40] The results revealed a strong synergistic effect among the three metals. The hollow structure and surface-folded nanosheets of this material increased active sites and specific surface areas, shortened charge transfer paths, and effectively improved electrochemical activity. Alternatively, NiCoMn-LDHs can be prepared by etching monometallic ZIF-67 templates with dual ions (Ni and Mn).[41] The amounts of Ni, Co, and Mn were optimized, and the Ni_2CoMn_1-LDH electrode exhibited superior specific capacitance.

Pristine LDH powder derived from MOF templates typically exhibits complex nanostructures, which partly enhance the conductivity and structural stability of the MOFs. Additionally, the 3D ordered structure provided by MOFs provides large surface areas and fast charge transport pathways.[42] However, its performance in energy storage applications remains suboptimal. Achieving desirable morphology, composition, and electrochemical performance requires careful control of the synthesis conditions.

3.2 LDH composites

Recent efforts have been focused on developing electrode materials with enhanced conductivity, capacity, and stability. While the uniformly ordered pore structure of MOFs offers adequate channels for electron and ion transport, the poor electrical conductivity of MOFs remains a significant challenge.[43,44] Though converting MOFs into LDHs can partially address these issues, pristine LDH powder still suffers from inadequate electron and ion transport. To enhance overall performance, researchers have explored assembling LDHs with carbon materials, conductive polymers, or metal/metal compounds to produce various LDH composites. Combining LDHs with conductive materials generates synergistic effects, resulting in attractive structural properties and new electrochemical advantages.[45]

3.2.1 Carbon materials. Carbon materials offer adjustable specific surface areas, excellent electrical conductivity, high chemical stability, and a wide operating temperature range.[46] Properly controlling the morphology of LDHs bound to carbon materials can effectively prevent LDH agglomeration and enhance the total surface area and conductivity.[47] Various carbon materials with different dimensions, including 0D carbon dots, 1D carbon nanotubes (CNTs) and carbon nanofibers (CNFs), 2D graphene oxide (GO) and graphitic carbon nitride (g-C_3N_4), and 3D carbon foams (CFs), have been composited with MOF-derived LDHs to improve their electrochemical performance.

As typical 0D carbon materials, carbon quantum dots (CQDs) exhibit favorable electronic properties and can serve as protective layers to stabilize electrode materials. Incorporating CQDs into LDHs stabilizes the interlamellar structure and shortens the charge transfer pathway, thereby enhancing the electrochemical properties of LDHs. For instance, Zhang *et al.* synthesized NiCo-LDH nanosheet-assembled hollow nanocages through regular etching of ZIF-67 with nickel nitrate and subsequently decorated p-type N-doped graphene quantum dots (N-GQDs) onto the surfaces of n-type NiCo-LDH nanosheets *via* the electrodeposition method.[48] The resulting N-GQD/H-NiCo-LDH composite exhibited superior specific capacitance (2347 F g^{-1} at 1 A g^{-1}) with ultrahigh rate performance (82% capacitance retention at 10 A g^{-1}) attributed to the enhanced electronic conductivity of N-GQDs and the provision of nitrogen-rich redox active sites. Additionally, the p–n heterojunction facilitated charge redistribution, enhancing the redox activity of the composite. In another study, CQDs were introduced during the synthesis of the Co-MOF, and the resulting CQDs/Co-MOF was transformed into porous CQDs/NiCo-LDHs *via* a solvothermal reaction.[49] The incorporation of CQDs induced strong electronic coupling between NiCo-LDHs and CQDs, thereby improving the reaction kinetics. Moreover, CQDs served as protective layers, mitigating volume changes during charge/discharge cycles.

CNTs are popular 1D carbon materials known for their high intrinsic conductivity and robust physical properties, including mechanical, chemical, and thermal stability.[50] Additionally, CNTs offer a large specific surface area, making them ideal scaffolds for supporting LDHs. Huang *et al.* introduced carboxylated CNTs during the *in situ* synthesis of the Ni–Co MOF, resulting in a hierarchical CNT/NiCo-LDH composite obtained through controlled alkaline hydrolysis of precursors (Fig. 4).[51] The incorporated CNTs served as electron transport channels within the LDHs and maintained the integrity of the active materials during the electrochemical process. The CNT/Ni–Co-LDH composite exhibited high specific capacitance (1628 F g^{-1} at 1 A g^{-1}), and the assembled hybrid supercapacitor demonstrated remarkable cycling stability (99.4% specific capacitance retention after 10 000 cycles).

2D carbon materials with unique lamellar structures, large surface areas, and ultrathin thicknesses have become an ideal platform for designing composite electrode materials. Among them, GO has garnered special attention due to its large lateral

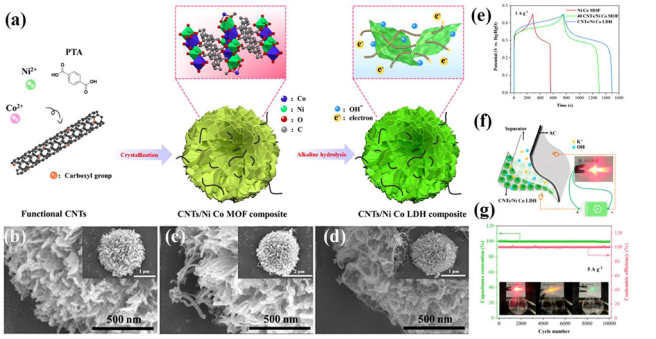

Fig. 4 (a) Schematic illustration of the synthesis process of the CNT/NiCo-LDH composite. SEM images of the as-synthesized (b) NiCo-MOF, (c) CNTs/NiCo-MOF and (d) CNTs/NiCo-LDH. (e) GCD curves of the as-prepared samples at 1 A g^{-1}. (f) Schematic illustration of the CNT/NiCo-LDH//AC hybrid supercapacitor. (g) Cycling performance and the coulombic efficiency of CNTs/NiCo-LDH//AC at 5 A g^{-1}. Reprinted with permission from ref. 51, Copyright 2021, Elsevier.

size, excellent electronic conductivity, and high stability.[52] Bai *et al.* reported a Co–Co LDH/GO composite, where GO nanosheets were initially sandwiched by ZIF-67 nanocages through facile co-deposition.[53] Subsequently, the ZIF-67 nanocages were converted into Co–Co LDH hollow nanocages *via* a thermal ion-exchange reaction with $Co(NO_3)_2{\cdot}6H_2O$. The Co–Co LDH/GO composite exhibited enhanced electrochemical properties compared to the Co–Co LDH alone, underscoring the crucial role of GO. Considering that the structural hardness of ZIF-8 is stronger than that of ZIF-67, improved cycling stability of the derived LDHs could be anticipated. To this end, GO/ZIF-8 was first prepared through a room-temperature aging process, and the ZIF-8 template was etched with nickel and cobalt nitrates (Fig. 5a).[54] The co-precipitation of zinc, cobalt, and nickel ions with the aid of hexamethylenetetramine resulted in the formation of Zn–Co–Ni LDH. The GO/Zn–Co–Ni LDH composite exhibited high specific capacitance, surpassing the composites of GO and binary LDHs (Fig. 5b).

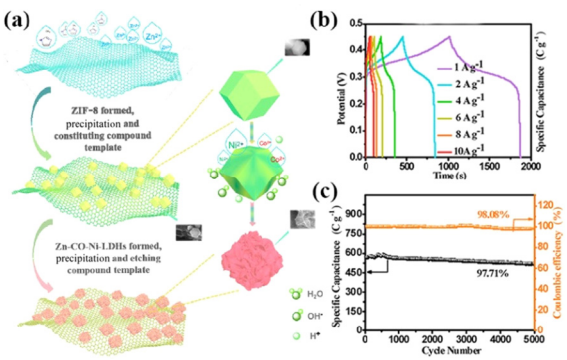

Fig. 5 (a) Schematic illustration of the synthesis of GO/Zn–Co–Ni LDH. (b) GCD curves of GO/Zn–Co–Ni LDH. (c) Cycling stability and coulombic efficiency of GO/Zn–Co–Ni LDH during 5000 cycles at 10 A g^{-1}. Reprinted with permission from ref. 54, Copyright 2020, American Chemical Society.

Furthermore, the GO/Zn–Co–Ni LDH demonstrated impressive cycling stability, retaining 97.7% of its capacitance after 5000 cycles at 10 A g^{-1} (Fig. 7c). MXene, a novel 2D transition metal carbide or carbonitride, is denoted as $M_{n+1}X_nT_x$, where M is an early transition metal, X is C and/or N, n = 1, 2, or 3, and T represents the terminal group (–O, –OH, and/or –F).[55] With its high electrical conductivity (6000–8000 S cm^{-1}) and good mechanical properties, MXene holds promise as an electrode material or additive to enhance the electrochemical performance of electrode materials.[56] Guo *et al.* synthesized MXene/NiCo-LDH composites by growing NiCo-ZIF-67 on an MXene substrate followed by alkaline hydrolysis using KOH.[57] The MXene substrate provided an efficient conductive network for electron transport, while the uniform anchoring of NiCo-LDH nanoparticles (NPs) on MXene offered a large surface area. Consequently, the prepared MXene/NiCo-LDH electrode exhibited a large specific capacitance (877 F g^{-1}) and outstanding cycling durability, with only a 9.1% capacitance loss after 30 000 cycles. The negatively charged terminal groups (–F, –OH, –O, *etc.*) of MXene could interact with positively charged materials. For instance, $Ti_3C_2T_x$ nanosheets (negatively charged) were assembled onto pre-prepared ZIF-67 (positively charged) to form sphere-like ZIF-67/$Ti_3C_2T_x$ nanocomposites through electrostatic effects.[22] After etching with $Ni(NO_3)_2{\cdot}6H_2O$, 3D porous flower-like NiCo-LDH/$Ti_3C_2T_x$ was obtained. NiCo-LDH/$Ti_3C_2T_x$-5 delivered a high specific capacity (635.7 C g^{-1} at 1 A g^{-1}) and good rate performance (60.1% at 20 A g^{-1}).

3D porous carbon materials, featuring interconnected conductive networks and large specific surface areas, serve as ideal substrates for encapsulating LDHs. For instance, Zhao *et al.* successfully prepared interconnected nanoporous carbon (INPC)/LDH composites.[58] They first grew ZIF-67 nanocages on the walls of an INPC framework derived from glucose as the carbon source, followed by obtaining NiCo-LDH nanosheet-assembled nanocages through controlled ion etching and co-deposition of ZIF-67. The resulting INPC/NiCo-LDH composite exhibited a higher specific capacitance compared to pure NiCo-LDH. Doping elements like nitrogen, oxygen, and fluorine into the carbon framework can further enhance the electrochemical performance. Liu *et al.* proposed a feasible strategy to anchor NiCo-LDH nanosheets onto 3D N-doped carbon foam (NCF).[59] Initially, Co-ZIF was deposited on NCF, prepared by calcining melamine foam, followed by transforming Co-ZIF into NiCo-LDH through a popular etching method. The NCF facilitated charge transfer and hindered the aggregation of NiCo-LDH nanosheets, providing abundant active sites. Consequently, the NiCo-LDH/NCF achieved a high specific capacity (975.6 C g^{-1} at 0.5 A g^{-1}), significantly larger than that of pristine NiCo-LDH.

Carbon materials with robust structures and tailorable morphologies serve as excellent conductive substrates for anchoring MOF-derived LDHs. However, the preparation of highly graphitized carbon demands significant energy consumption. Moreover, to enhance compatibility with MOFs, carbon materials often undergo a functionalization process, which may not be environmentally friendly.

3.2.2 Conductive polymers. Recently, conductive polymers (CPs) such as polypyrrole (PPy),[60] polyaniline (PANI)[61] and poly(3,4-ethylenedioxythiophene) (PEDOT)[62] have found wide applications as electrode materials for SCs owing to their high electrical conductivity, rapid redox processes, and adjustable redox activity. Compared with carbon materials, CPs can be simply prepared by straightforward and economical polymerization methods. CPs contain a large number of hydrophilic functional groups, which are beneficial for the nucleation and growth of MOF crystals. Additionally, the good wettability of CPs facilitates electrolyte penetration and rapid ion transport. Thus, CPs are promising conductive substrates for coupling with LDHs, and the resulting composites could combine the advantages of CPs and LDHs. For example, ZIF-67 dodecahedra were uniformly strung on inter-crosslinked PPy tubes *via in situ* synthesis, and ZIF-67 was converted into NiCo-LDH through the etching and co-precipitation processes with Ni$(NO_3)_2{\cdot}6H_2O$.[60] Their electrochemical properties can be further optimized by sulfidation to NiCoS. Benefiting from the advantages of MOF derivatives with porous structures and PPy tubes providing rapid electron transfer pathways, the resultant composite electrodes showed ultra-high specific capacitance and excellent rate performance. In another study, NiCo-LDH nanosheet-assembled hollow nanocages were first grown on carbon cloth (CC) using ZIF-67 as the template.[62] Subsequently, an ultrathin PEDOT layer was coated onto NiCo LDH through an electrodeposition process to generate the PEDOT@NiCo-LDH/CC composite (Fig. 6). The incorporation of PEDOT could improve conductivity and also prevent the destruction of the LDH during the electrochemical process. As a result, the PEDOT@NiCo-LDH/CC electrode showed high specific capacitance (1508 F g^{-1} at 1 A g^{-1}), good rate capability (71.9% at 20 A g^{-1}), and remarkable cycling durability (90.1% capacitance retention after 10 000 cycles at 20 A g^{-1}).

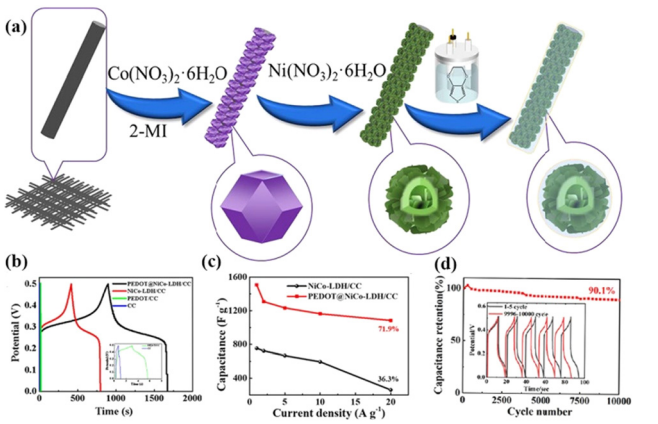

Fig. 6 (a) Schematic illustration of the preparation of PEDOT@NiCo-LDH/CC. (b) GCD curves of the samples at 1 A g^{-1}. (c) Corresponding capacitance at different current densities. (d) Cycling properties of PEDOT@NiCo-LDH/CC at 20 A g^{-1} over 10 000 cycles (inset: GCD curves of the first and last 5 cycles). Reprinted with permission from ref. 62, Copyright 2023, Elsevier.

The ease of synthesis and the presence of abundant hydrophilic functional groups in CPs make them suitable for coupling with MOFs, enabling the fabrication of composites of CPs and MOF-derived LDHs. In such composites, the agglomeration of LDHs can be effectively inhibited, while CPs offer efficient pathways for electron transport, significantly enhancing electrical conductivity. However, they are susceptible to volume expansion and structural damage during the electrochemical process.[63] The key to success lies in constructing composites with well-defined compositions and nanostructures to improve overall performance.

3.2.3 Transition metal/metal compounds. Although carbon materials and conductive polymers have been widely utilized as frameworks for supporting MOF-derived LDHs, they are hindered by either complex construction and functionalization processes or degradation in alkaline electrolyte solutions. Moreover, they contribute less to the overall capacitance due to fewer redox reaction sites. Transition metal compounds such as metal oxides, sulfides, phosphides and selenides with rich redox reactions offer superior electrical conductivity, mechanical strength, and thermal stability compared to LDHs. Consequently, significant efforts have been directed towards enhancing the electrochemical properties of LDHs by constructing composites of transition metal compounds and LDHs.[64] In comparison with LDHs, metal sulfides possess higher conductivity owing to their lower energy band gaps. Thus, the rate capability and cycling stability of LDHs can be enhanced by combining them with metal sulfides. Guan *et al.* synthesized CoS_x/Ni–Co LDH composites by employing ZIF-67 as the template.[65] They first partially sulfurized ZIF-67 using thioacetamide to form CoS_x NPs around ZIF-67, followed by etching with nickel nitrate to form Ni–Co LDH nanosheets on the surface of CoS_x (Fig. 7a). By harnessing the advantages of both metal sulfides and LDH, the CoS_x/Ni–Co LDH composite exhibited a high specific capacitance of 1562 F g^{-1} at 1 A g^{-1}. Metal oxides such as MnO_2, Co_3O_4, and NiO are also commonly employed as active materials for SCs due to their high theoretical capacitance, low cost, and environmental friendliness. Wang *et al.* utilized MnO_2 nanotubes to assemble NiCo-LDH nanocages decorated with CoS_2 NPs, which were derived from the ZIF-67 template (Fig. 7b).[66] The resulting 1D hierarchical nanostructure provided large electroactive sites and prevented the collapse of the nanocages. Additionally, the incorporation of CoS_2 NPs enhanced electrical conductivity and structural stability, resulting in the nanocomposite exhibiting a high specific capacitance of 1547 F g^{-1} at 1 A g^{-1} and excellent rate performance (76.9% at 10 A g^{-1}). Various forms of transition metals, including Ag nanowires,[67] Ni nanowires,[68] and Ni and Co particles,[69] have been combined with LDHs to enhance the electrochemical performance of electrode materials.

In particular, Ag, known for its high electronic conductivity (6.3 × 107 S m^{-1}), has garnered significant attention. Guan and colleagues reported the synthesis of C, N, Ag-doped NiCoMn-LDH (C/N-CNMA) using ZIF-67 as the precursor (Fig. 7c).[70] The incorporation of Ag modulated the crystallinity

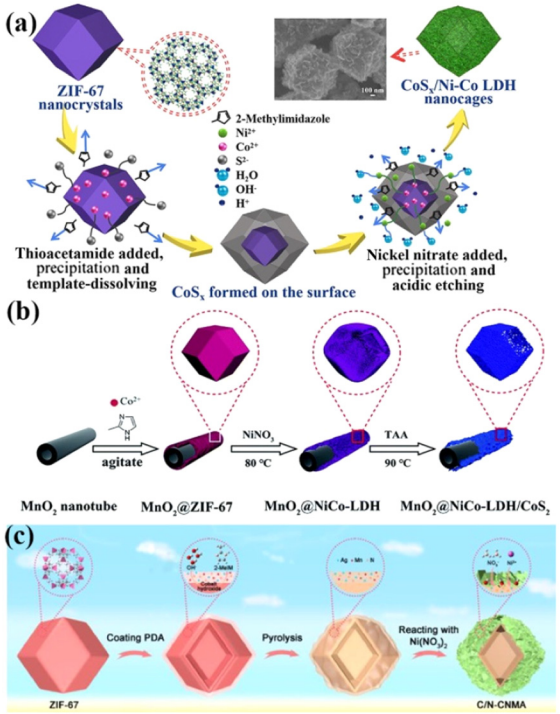

Fig. 7 (a) Schematic illustration depicting the preparation of CoS_x/Ni–Co LDH composites. Reprinted with permission from ref. 65, Copyright 2019, Elsevier. (b) Schematic diagram outlining the synthesis of MnO_2@NiCo-LDH/CoS_2. Reprinted with permission from ref. 66, Copyright 2019, the Royal Society of Chemistry. (c) Schematic illustration demonstrating the synthesis of C/N-CNMA. Reprinted with permission from ref. 70, Copyright 2023, Elsevier.

and electronic structure of the LDH, resulting in improved conductivity, active sites, and electrochemical activity. C/N-CNMA exhibited a high specific capacitance of 1988 F g^{-1} at 1 A g^{-1}.

In summary, previous studies have demonstrated several advantages of LDH composites: (1) these composites can harness the synergistic effects of individual components, leading to enhanced overall performance.[71] (2) By combining LDHs with other materials, such as core–shell structures, the resulting composites can exhibit hierarchical and specific structures that provide additional active sites, consequently increasing the specific capacitance of the materials.[72] (3) In such composites, dispersion and structural stability are typically improved. However, challenges arise in controlling the coupling process, which can result in pore blocking and hindered ion transport. Moreover, achieving the optimal synergistic effect requires careful control over the proportionality between the components. An appropriate amount can increase electrical conductivity, while an excessive amount may lead to adverse effects.[73]

3.3 LDH-based arrays

Despite the great promise of MOF-derived LDHs and their composites in SCs, the powdery nature of electrode materials necessitates casting them onto current collectors using insulat-

ing polymer binders and conductive additives. Unfortunately, this process increases interfacial resistance and reduces the number of electroactive sites. Therefore, there is growing interest in preparing free-standing MOF-derived LDH arrays on conductive substrates without the need for binders and additives. Two common strategies are employed for constructing MOF-derived LDH arrays. One approach involves depositing MOF crystals on metal compound arrays, followed by the conversion of the MOF into LDH. This method allows for the fabrication of complex hierarchical LDH-based arrays. For instance, Bi *et al.* utilized CuO nanorod arrays as the supporting skeleton for ZIF-67, constructing a hierarchical CuO@NiCo-LDH nanoarray on copper foam (CF) after converting ZIF-67 into NiCo-LDH (Fig. 8a–i).[74] The binder-free CuO nanorods with good conductivity facilitated rapid electron transfer paths between NiCo-LDH nanocages, while anchoring NiCo-LDH nanocages on CuO nanorods enhanced structural stability. Consequently, CuO@NiCo-LDH/CF exhibited high areal capacitance (5607 mF cm^{-2} at 1 mA cm^{-2}) and remarkable cycle life (only 6.9% capacitance loss after 5000 cycles at 20 mA cm^{-2}). Similarly, Lei *et al.* fabricated CuO/CF@NiCoMn-OH nanoarrays using CuO/CF@ZIF-67 as the template.[75] The ternary LDH possessed variable valence states for redox reactions, and its unique structure facilitated charge transport, resulting in remarkable specific capacity (26.8 F cm^{-2} at 8 mA cm^{-2}).

Another strategy for constructing MOF-derived LDH arrays involves the direct growth of MOF arrays on conductive substrates, followed by the transformation of the MOF into LDH. Unlike 3D ZIF-8 and ZIF-67, 2D ZIF-L exhibits a unique leaf-like morphology with customizable compositions, making it an ideal template for designing various array electrodes. For instance, bimetallic CuCo-ZIF-L arrays were synthesized on carbon cloth (CC) *via in situ* synthesis, yielding ternary CuCoNi-OH with abundant in-plane pores through a high-temperature etching process (Fig. 9).[76] The 2D porous nanosheet arrays effectively increased the surface area, and the introduction of Cu into NiCo-LDH enhanced conductivity. Owing to these advantages, CuCoNi-OH demonstrated high specific capacity (821.6 C g^{-1} at 1 A g^{-1}) and excellent rate performance (89.8% at 20 A g^{-1}), as shown in Fig. 9d. Besides, a hybrid supercapacitor device using the CuCoNi-OH electrode coupled with the HPC electrode exhibited outstanding cycling stability (Fig. 9h).

The direct construction of MOF-derived LDH nanostructures on conductive substrates offers improved electronic conductivity and prevents the aggregation of active materials, resulting in enhanced electrochemical performance compared to powdery electrode materials. Further optimization of the electrochemical performance can be achieved by tuning the

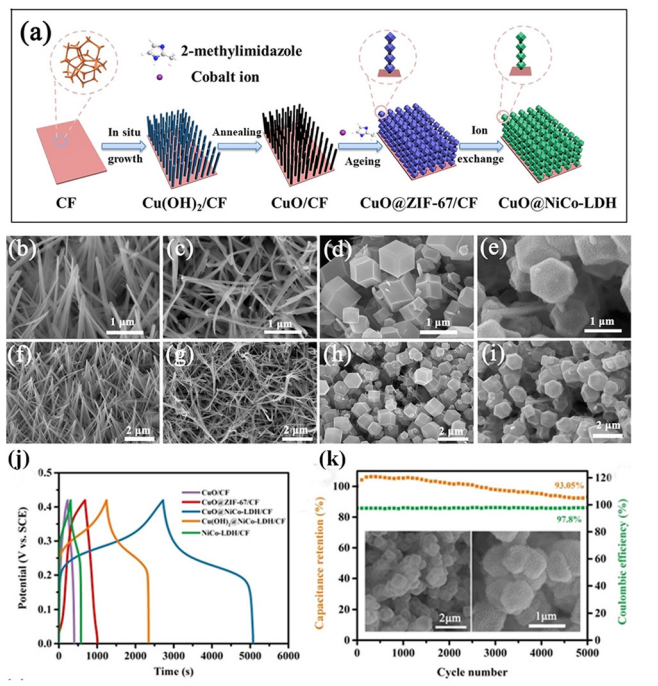

Fig. 8 (a) Schematic showing the construction of CuO@NiCo-LDH/CF. SEM images of (b and f) $Cu(OH)_2$, (c and g) CuO, (d and h) CuO@ZIF-67 and (e and i) CuO@NiCo-LDH on CF. (j) GCD curves at different current densities of CuO@NiCo-LDH/CF, and (k) cycling stability and coulombic efficiency of CuO@NiCo-LDH/CF during 5000 cycles (the inset shows the SEM images of CuO@NiCo-LDH/CF before and after cycling). Reprinted with permission from ref. 74, Copyright 2022, WILEY-VCH.

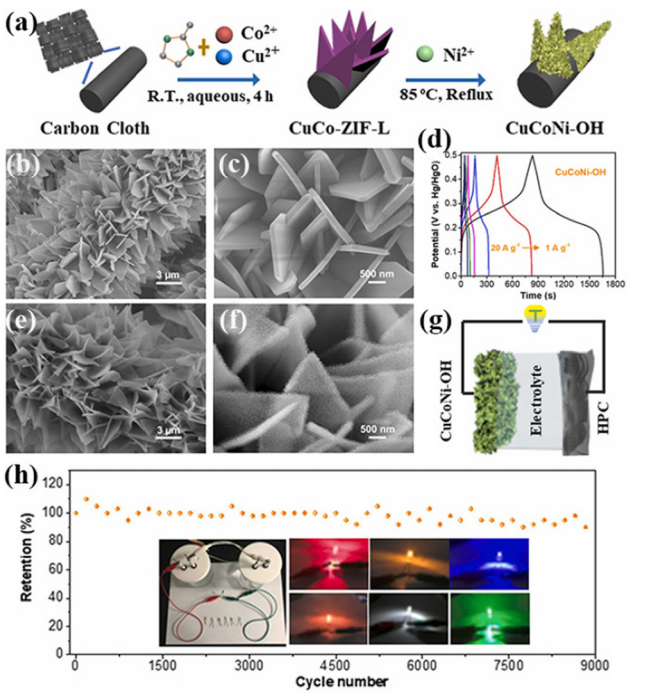

Fig. 9 (a) Schematic of the synthesis procedure of CuCo-ZIF-L and CuCoNi-OH. (b and c) SEM images of CuCo-ZIF-L. (d) GCD curves of the CuCoNi-OH electrode at different current densities. (e and f) SEM images of CuCoNi-OH. (g) Schematic illustration of the hybrid supercapacitor device using the CuCoNi-OH electrode coupled with the HPC electrode and (h) cycling performance of the hybrid supercapacitor device at 3.3 A g^{-1}. The inset of (h) shows the photographic images of two serially connected hybrid devices lighting up different color LEDs. Reprinted with permission from ref. 76, Copyright 2022, Elsevier.

compositions, defects, and morphologies of the electrode materials.[77,78]

4 Summary and outlook

MOFs are rapidly emerging as promising electrode materials in the realm of energy storage, owing to their chemical versatility and tunability. Nevertheless, their instability in electrolytes and poor electronic conductivity retard their applications. Fortunately, MOF-derived LDHs exhibit enhanced stability and conductivity, catering to the requirements of various applications. Typically, two strategies are employed to convert MOF templates into LDHs: the hydrolysis strategy involves substituting organic ligands with OH^- in alkaline media, while the etching strategy entails acidic etching of MOFs followed by co-precipitation. Constructing 3D-structured LDHs from MOFs circumvents the stacking issue of LDHs and exposes more active sites, thereby improving structural stability and electronic conductivity. Furthermore, coupling MOF-derived LDHs with electrically conductive materials such as carbon materials, conductive polymers, and metal/metal compounds significantly enhances composite performance. LDH-based arrays offer notable advantages over powdery electrode materials due to their aligned nanostructures and absence of "dead volume". Despite the great progress that has been made, several challenges and prospects coexist. Firstly, issues like MOF collapse and uncontrolled LDH growth need to be addressed through *operando* characterization studies to elucidate transformation mechanisms. Secondly, careful control of synthesis parameters is essential to prevent aggregation and porosity loss when coupling MOF-derived LDH powders with other electrode materials. Impressively, MOF-templated LDH nanoarrays exhibit remarkable advantages over powders owing to their oriented structure. Thirdly, while MOF-derived LDHs often exhibit high capacity, their rate performance and cycle life are suboptimal. Strategies such as defect engineering, interlayer space regulation, and heterojunction construction could enhance electrochemical performance. Lastly, the specific capacity of MOF-derived LDHs in two-electrode devices is lower than that in three-electrode systems. Therefore, the design of negative electrode materials, electrolyte selection, and device assembly methods must be carefully considered to achieve high energy storage properties.

Author contributions

Fujuan Luo: writing – original draft. Xiaoguang San: writing – review & editing. Yisong Wang: writing – review & editing. Dan Meng: writing – review & editing. Kai Tao: conceptualization, supervision and writing – review & editing.

Conflicts of interest

There are no conflicts to declare.

Acknowledgements

This work was financially supported by the Key Project in Science & Technology of SYUCT (No. 2023DB005), the Natural Science Foundation of Liaoning Province (No. 2023-MS-235 and 2023-MSLH-270), the Liaoning Educational Department Foundation (No. LJKMZ20220762 and JYTMS20231510), and the Natural Science Foundation of Ningbo (2022J094).

References

1 Y. Sun, J. Sun, J. S. Sanchez, Z. Xia, L. Xiao, R. Chen and V. Palermo, Surface chemistry and structure manipulation of graphene-related materials to address the challenges of electrochemical energy storage, *Chem. Commun.*, 2023, **59**(18), 2571–2583.
2 C. Li, Y. Yuan, M. Yue, Q. Hu, X. Ren, B. Pan, C. Zhang, K. Wang and Q. Zhang, Recent Advances in Pristine Iron Triad Metal-Organic Framework Cathodes for Alkali Metal-Ion Batteries, *Small*, 2024, 2310373.
3 N. Raza, T. Kumar, V. Singh and K.-H. Kim, Recent advances in bimetallic metal-organic framework as a potential candidate for supercapacitor electrode material, *Coord. Chem. Rev.*, 2021, **430**, 213660.
4 R. Kumar, S. Sahoo, E. Joanni, R. Pandey and J.-J. Shim, Vacancy designed 2D materials for electrodes in energy storage devices, *Chem. Commun.*, 2023, **59**(41), 6109–6127.
5 S. Deka, Nanostructured mixed transition metal oxide spinels for supercapacitor applications, *Dalton Trans.*, 2023, **52**(4), 839–856.
6 L. Zhang, J. Sun, F. Li, Z. Cao, J. Lang and S. Li, Manganese–cobalt hydroxide nanosheets anchored on a hollow sulfur-doped bimetallic MOF for high-performance supercapacitors and the hydrogen evolution reaction in alkaline media, *Dalton Trans.*, 2024, **53**(3), 1274–1283.
7 F. H. Gourji, T. Rajaramanan, Ø. Frette and D. Velauthapillai, Fabrication of ternary NiCoMoOx with yolk–shell hollow structure as a positive electrode material for high-performance electrochemical capacitor applications, *Nanoscale*, 2023, **15**(39), 16178–16187.
8 Q. Pan, F. Zheng, D. Deng, B. Chen and Y. Wang, Interlayer Spacing Regulation of NiCo-LDH Nanosheets with Ultrahigh Specific Capacity for Battery-Type Supercapacitors, *ACS Appl. Mater. Interfaces*, 2021, **13**(47), 56692–56703.
9 Y. Guo, X. Hong, Y. Wang, Q. Li, J. Meng, R. Dai, X. Liu, L. He and L. Mai, Multicomponent Hierarchical Cu-Doped NiCo-LDH/CuO Double Arrays for Ultralong-Life Hybrid Fiber Supercapacitor, *Adv. Funct. Mater.*, 2019, **29**(24), 1809004.
10 T. Li, X. Hu, C. Yang, L. Han and K. Tao, A heterostructure of NiMn-LDH nanosheets assembled on ZIF-L-derived ZnCoS hollow nanosheets with a built-in electric field enables boosted electrochemical energy storage, *Dalton Trans.*, 2023, **52**(45), 16640–16649.

11 J. Shi, H. Tai, D. Xu, X. Kang and Z. Liu, Efficient improvement in the electrochemical performance of petal-like lamellar NiMn–LDHs with affluent oxygen vacancies derived from Mn MOF-74, *Dalton Trans.*, 2024, **53**(7), 3167–3179.
12 Y. Liu, C. Zhang, Q. Cai, J. Zhang and Z. Zheng, A moderate method for in situ growing Fe-based LDHs on Ni foam for catalyzing the oxygen evolution reaction, *Nanoscale*, 2023, **15**(47), 19322–19329.
13 J. L. Obeso, J. G. Flores, C. V. Flores, M. T. Huxley, J. A. de los Reyes, R. A. Peralta, I. A. Ibarra and C. Leyva, MOF-based catalysts: insights into the chemical transformation of greenhouse and toxic gases, *Chem. Commun.*, 2023, **59**(68), 10226–10242.
14 Y. Shi, B. Zhu, X. Guo, W. Li, W. Ma, X. Wu and H. Pang, MOF-derived metal sulfides for electrochemical energy applications, *Energy Storage Mater.*, 2022, **51**, 840–872.
15 X. Zhao, K. Tao and L. Han, Self-supported metal–organic framework-based nanostructures as binder-free electrodes for supercapacitors, *Nanoscale*, 2022, **14**(6), 2155–2166.
16 S. A. Al Kiey and H. N. Abdelhamid, Metal-organic frameworks (MOFs)-derived Co3O4@N-doped carbon as an electrode materials for supercapacitor, *J. Energy Storage*, 2022, **55**, 105449.
17 H. N. Abdelhamid, S. A. Al Kiey and W. Sharmoukh, A high-performance hybrid supercapacitor electrode based on ZnO/nitrogen-doped carbon nanohybrid, *Appl. Organomet. Chem.*, 2022, **36**(1), e6486.
18 J. Chen and J. Qian, Insights on MOF-derived metal–carbon nanostructures for oxygen evolution, *Dalton Trans.*, 2024, **53**(7), 2903–2916.
19 G. Wang, D. Huang, M. Cheng, S. Chen, G. Zhang, L. Lei, Y. Chen, L. Du, R. Li and Y. Liu, Metal-organic frameworks template-directed growth of layered double hydroxides: A fantastic conversion of functional materials, *Coord. Chem. Rev.*, 2022, **460**, 214467.
20 Y. Xue, S. Zheng, H. Xue and H. Pang, Metal–organic framework composites and their electrochemical applications, *J. Mater. Chem. A*, 2019, **7**(13), 7301–7327.
21 F. Parsapour, M. Moradi and A. Bahadoran, Metal-organic frameworks-derived layered double hydroxides: From controllable synthesis to various electrochemical energy storage/conversion applications, *Adv. Colloid Interface Sci.*, 2023, **313**, 102865.
22 Y. Wang, C. Shi, Y. Chen, D. Li, G. Wu, C. Wang and L. Guo, 3D flower-like MOF-derived NiCo-LDH integrated with Ti3C2Tx for high-performance pseudosupercapacitors, *Electrochim. Acta*, 2021, **376**, 138040.
23 W. Wang, H. Yan, U. Anand and U. Mirsaidov, Visualizing the Conversion of Metal–Organic Framework Nanoparticles into Hollow Layered Double Hydroxide Nanocages, *J. Am. Chem. Soc.*, 2021, **143**(4), 1854–1862.
24 D. Cai, Z. Yang, R. Tong, H. Huang, C. Zhang and Y. Xia, Binder-Free MOF-Based and MOF-Derived Nanoarrays for Flexible Electrochemical Energy Storage: Progress and Perspectives, *Small*, 2024, **20**(12), 2305778.
25 K. Makgopa, M. S. Ratsoma and K. D. Modibane, Intrinsic properties of metal–organic frameworks (MOFs) in supercapacitor applications, *Curr. Opin. Electrochem.*, 2022, **36**, 101112.
26 R. Rajak, R. Kumar, S. N. Ansari, M. Saraf and S. M. Mobin, Recent highlights and future prospects on mixed-metal MOFs as emerging supercapacitor candidates, *Dalton Trans.*, 2020, **49**(34), 11792–11818.
27 X.-W. Liu, T.-J. Sun, J.-L. Hu and S.-D. Wang, Composites of metal–organic frameworks and carbon-based materials: preparations, functionalities and applications, *J. Mater. Chem. A*, 2016, **4**(10), 3584–3616.
28 H. Zhang, B. Xu, Z. Xiao, H. Mei, L. Zhang, Y. Han and D. Sun, Optimizing crystallinity and porosity of hierarchical $Ni(OH)_2$ through conformal transformation of metal–organic framework template for supercapacitor applications, *CrystEngComm*, 2018, **20**(30), 4313–4320.
29 Z. Xiao, Y. Mei, S. Yuan, H. Mei, B. Xu, Y. Bao, L. Fan, W. Kang, F. Dai, R. Wang, L. Wang, S. Hu, D. Sun and H.-C. Zhou, Controlled Hydrolysis of Metal–Organic Frameworks: Hierarchical Ni/Co-Layered Double Hydroxide Microspheres for High-Performance Supercapacitors, *ACS Nano*, 2019, **13**(6), 7024–7030.
30 H. Zhang, B. Xu, H. Mei, Y. Mei, S. Zhang, Z. Yang, Z. Xiao, W. Kang and D. Sun, "HOT" Alkaline Hydrolysis of Amorphous MOF Microspheres to Produce Ultrastable Bimetal Hydroxide Electrode with Boosted Cycling Stability, *Small*, 2019, **15**(49), 1904663.
31 H. Chen, L. Hu, M. Chen, Y. Yan and L. Wu, Nickel–Cobalt Layered Double Hydroxide Nanosheets for High–performance Supercapacitor Electrode Materials, *Adv. Funct. Mater.*, 2013, **24**(7), 934–942.
32 Z. Jiang, Z. Li, Z. Qin, H. Sun, X. Jiao and D. Chen, LDH nanocages synthesized with MOF templates and their high performance as supercapacitors, *Nanoscale*, 2013, **5**(23), 11770–11775.
33 J. Cao, S. Sun, X. Li, Z. Yang, W. Xiong, Y. Wu, M. Jia, Y. Zhou, C. Zhou and Y. Zhang, Efficient charge transfer in aluminum-cobalt layered double hydroxide derived from Co-ZIF for enhanced catalytic degradation of tetracycline through peroxymonosulfate activation, *Chem. Eng. J.*, 2020, **382**, 122802.
34 E. Bao, X. Ren, Y. Wang, Z. Zhang, C. Luo, X. Liu, C. Xu and H. Chen, Advanced hybrid supercapacitors assembled with CoNi LDH nanoflowers and nanosheets as high-performance cathode materials, *J. Energy Storage*, 2024, **82**, 110535.
35 T.-H. Gu, N. H. Kwon, K.-G. Lee, X. Jin and S.-J. Hwang, 2D inorganic nanosheets as versatile building blocks for hybrid electrode materials for supercapacitor, *Coord. Chem. Rev.*, 2020, **421**, 213439.
36 X. Liu, L. Zhang, X. Gao, C. Guan, Y. Hu and J. Wang, Enlarged Interlayer Spacing in Cobalt–Manganese Layered Double Hydroxide Guiding Transformation to Layered Structure for High Supercapacitance, *ACS Appl. Mater. Interfaces*, 2019, **11**(26), 23236–23243.

37 R. Ramachandran, Y. Lan, Z.-X. Xu and F. Wang, Construction of NiCo-Layered Double Hydroxide Microspheres from Ni-MOFs for High-Performance Asymmetric Supercapacitors, *ACS Appl. Energy Mater.*, 2020, **3**(7), 6633–6643.
38 J. Hu, Z. Wu, Z. Sun, S. Lu, T. Guo, W. Yang, Q. Xie and Y. Ruan, Nanostructured Mn-Doped Ni–Co Hydroxide Microspheres for Fast-Kinetics Supercapacitors, *ACS Appl. Nano Mater.*, 2024, **7**(3), 3269–3278.
39 X. Zheng, X. Han, X. Zhao, J. Qi, Q. Ma, K. Tao and L. Han, Construction of Ni-Co-Mn layered double hydroxide nanoflakes assembled hollow nanocages from bimetallic imidazolate frameworks for supercapacitors, *Mater. Res. Bull.*, 2018, **106**, 243–249.
40 J. Dai, Z. Li, R. Yu and D. Huang, MOFs as template-derived NiCoMn-LDH with a hollow polyhedron structure for high-performance supercapacitors, *J. Alloys Compd.*, 2023, **936**, 168313.
41 Y. Chen, J. Yang, H. Yu, J. Zeng, G. Li, B. Chang, C. Wu, X. Guo, G. Chen, L. Zheng and X. Wang, Design and Preparation of NiCoMn Ternary Layered Double Hydroxides with a Hollow Dodecahedral Structure for High-Performance Asymmetric Supercapacitors, *ACS Appl. Energy Mater.*, 2022, **5**(6), 6772–6782.
42 M. A. Tahir, N. Arshad and M. Akram, Recent advances in metal organic framework (MOF) as electrode material for super capacitor: A mini review, *J. Energy Storage*, 2022, **47**, 103530.
43 S. Sanati, R. Abazari, J. Albero, A. Morsali, H. García, Z. Liang and R. Zou, Metal–Organic Framework Derived Bimetallic Materials for Electrochemical Energy Storage, *Angew. Chem., Int. Ed.*, 2020, **60**(20), 11048–11067.
44 Y. He, Z. Yin, Z. Wang, H. Wang, W. Xiong, B. Song, H. Qin, P. Xu and G. Zeng, Metal-organic frameworks as a good platform for the fabrication of multi-metal nanomaterials: design strategies, electrocatalytic applications and prospective, *Adv. Colloid Interface Sci.*, 2022, **304**, 102668.
45 X. Gao, P. Wang, Z. Pan, J. P. Claverie and J. Wang, Recent Progress in Two–Dimensional Layered Double Hydroxides and Their Derivatives for Supercapacitors, *ChemSusChem*, 2020, **13**(6), 1226–1254.
46 H. Jiang, P. S. Lee and C. Li, 3D carbon based nanostructures for advanced supercapacitors, *Energy Environ. Sci.*, 2013, **6**(1), 41–53.
47 R. Kumar, E. Joanni, S. Sahoo, J.-J. Shim, W. K. Tan, A. Matsuda and R. K. Singh, An overview of recent progress in nanostructured carbon-based supercapacitor electrodes: From zero to bi-dimensional materials, *Carbon*, 2022, **193**, 298–338.
48 C. Zhang, L. Zhang, Q. Liu, Y. Ding, L. Cheng, M. Wu and Z. Li, Enhanced interfacial electron transfer by constructing NiCo-LDH hollow nanocages decorated N-doped graphene quantum dots heterojunction for high-performance supercapacitors, *Appl. Surf. Sci.*, 2022, **602**, 154352.
49 W. Luo, W. Chen, H. Quan, Z.-X. Zhang, Y. Zeng, Y. Wang and D. Chen, Strongly coupled carbon quantum dots/NiCo-LDHs nanosheets on carbon cloth as electrode for high performance flexible supercapacitors, *Appl. Surf. Sci.*, 2022, **591**, 153161.
50 F. Mashkoor, M. Shoeb, M. N. Khan and C. Jeong, CNT supported Sm/Co-LDH for antimony adsorption and subsequent application in supercapacitor to prevent secondary pollution, *J. Aolloys Compd.*, 2024, **981**, 173557.
51 M. Huang, Y. Wang, J. Chen, D. He, J. He and Y. Wang, Biomimetic design of Ni Co LDH composites linked by carbon nanotubes with plant conduction tissues characteristic for hybrid supercapacitors, *Electrochim. Acta*, 2021, **381**, 138289.
52 G. Wang, Y. Ma, J. Wang, P. Lu, Y. Wang and Z. Fan, Metal functionalization of two-dimensional nanomaterials for electrochemical carbon dioxide reduction, *Nanoscale*, 2023, **15**(14), 6456–6475.
53 X. Bai, J. Liu, Q. Liu, R. Chen, X. Jing, B. Li and J. Wang, *In situ* Fabrication of MOF-Derived Co—Co Layered Double Hydroxide Hollow Nanocages/Graphene Composite: A Novel Electrode Material with Superior Electrochemical Performance, *Chem. – Eur. J.*, 2017, **23**(59), 14839–14847.
54 L. Zhu, C. Hao, X. Wang and Y. Guo, Fluffy Cotton-Like GO/Zn–Co–Ni Layered Double Hydroxides Form from a Sacrificed Template GO/ZIF-8 for High Performance Asymmetric Supercapacitors, *ACS Sustainable Chem. Eng.*, 2020, **8**(31), 11618–11629.
55 D. Xu, Z. Zhang, K. Tao and L. Han, A heterostructure of a 2D bimetallic metal–organic framework assembled on an MXene for high-performance supercapacitors, *Dalton Trans.*, 2023, **52**(8), 2455–2462.
56 K. Nasrin, V. Sudharshan, K. Subramani and M. Sathish, Insights into 2D/2D MXene Heterostructures for Improved Synergy in Structure toward Next-Generation Supercapacitors: A Review, *Adv. Funct. Mater.*, 2022, **32**(18), 2110267.
57 H. Guo, J. Zhang, M. Xu, M. Wang, F. Yang, N. Wu, T. Zhang, L. Sun and W. Yang, Zeolite-imidazole framework derived nickel-cobalt hydroxide on ultrathin MXene nanosheets for long life and high performance supercapacitance, *J. Alloys Compd.*, 2021, **888**, 161250.
58 K. Zhao, Z. Wang, X. Sun, H. Guo, H. Fu, Z. Lu, Z. Liu and J. Liu, Metal-organic framework derived nickel-cobalt layered double hydroxide nanosheets cleverly constructed on interconnected nano-porous carbon for high-performance supercapacitors, *J. Energy Storage*, 2023, **60**, 106559.
59 Y. Liu, Y. Wang, C. Shi, Y. Chen, D. Li, Z. He, C. Wang, L. Guo and J. Ma, Co-ZIF derived porous NiCo-LDH nanosheets/N doped carbon foam for high-performance supercapacitor, *Carbon*, 2020, **165**, 129–138.
60 X. Zhao, Q. Ma, K. Tao and L. Han, ZIF-Derived Porous CoNi2S4 on Intercrosslinked Polypyrrole Tubes for High-Performance Asymmetric Supercapacitors, *ACS Appl. Energy Mater.*, 2021, **4**(4), 4199–4207.
61 L. Wang, X. Feng, L. Ren, Q. Piao, J. Zhong, Y. Wang, H. Li, Y. Chen and B. Wang, Flexible Solid-State Supercapacitor Based on a Metal–Organic Framework Interwoven by

Electrochemically-Deposited PANI, *J. Am. Chem. Soc.*, 2015, **137**(15), 4920–4923.

62 J. Zou, J. Zou, W. Zhong, Q. Liu, X. Huang, Y. Gao, L. Lu and S. Liu, PEDOT coating boosted NiCo-LDH nanocage on CC enable high-rate and durable pseudocapacitance reaction, *J. Electroanal. Chem.*, 2023, **928**, 117069.

63 Y. Yuan, J. Zhou, M. I. Rafiq, S. Dai, J. Tang and W. Tang, Growth of NiMn layered double hydroxide and polypyrrole on bacterial cellulose nanofibers for efficient supercapacitors, *Electrochim. Acta*, 2019, **295**, 82–91.

64 P. Zhou, C. Wang, Y. Liu, Z. Wang, P. Wang, X. Qin, X. Zhang, Y. Dai, M.-H. Whangbo and B. Huang, Sulfuration of NiV-layered double hydroxide towards novel supercapacitor electrode with enhanced performance, *Chem. Eng. J.*, 2018, **351**, 119–126.

65 X. Guan, M. Huang, L. Yang, G. Wang and X. Guan, Facial design and synthesis of CoSx/Ni-Co LDH nanocages with rhombic dodecahedral structure for high-performance asymmetric supercapacitors, *Chem. Eng. J.*, 2019, **372**, 151–162.

66 X. Wang, F. Huang, F. Rong, P. He, R. Que and S. P. Jiang, Unique MOF-derived hierarchical MnO_2 nanotubes@NiCo-LDH/CoS2 nanocage materials as high performance supercapacitors, *J. Mater. Chem. A*, 2019, **7**(19), 12018–12028.

67 S. C. Sekhar, G. Nagaraju and J. S. Yu, Conductive silver nanowires-fenced carbon cloth fibers-supported layered double hydroxide nanosheets as a flexible and binder-free electrode for high-performance asymmetric supercapacitors, *Nano Energy*, 2017, **36**, 58–67.

68 A. Mahieddine and L. Adnane-Amara, Fabrication of hierarchical Ni nanowires@ NiCo-layered double hydroxide nanosheets core-shell hybrid arrays for high-performance hybrid supercapacitors, *Electrochim. Acta*, 2023, **439**, 141622.

69 Y. Liu, N. Fu, G. Zhang, M. Xu, W. Lu, L. Zhou and H. Huang, Design of Hierarchical Ni-Co@Ni-Co Layered Double Hydroxide Core–Shell Structured Nanotube Array for High-Performance Flexible All-Solid-State Battery-Type Supercapacitors, *Adv. Funct. Mater.*, 2017, **27**(8), 1605307.

70 X. Guan, J. Chen, E. Zhu, P. Yin, L. Yang, X. Guan and G. Wang, Intrinsic electrochemical activity modulation of MOF-derived C/N-NiCoMn-LDH/Ag electrode for low temperature hybrid supercapacitors, *J. Mater. Sci. Technol.*, 2023, **150**, 145–158.

71 C. Guan, X. Li, Z. Wang, X. Cao, C. Soci, H. Zhang and H. J. Fan, Nanoporous Walls on Macroporous Foam: Rational Design of Electrodes to Push Areal Pseudocapacitance, *Adv. Mater.*, 2012, **24**(30), 4186–4190.

72 F. Zhu, W. Liu, Y. Liu and W. Shi, Construction of porous interface on CNTs@NiCo-LDH core-shell nanotube arrays for supercapacitor applications, *Chem. Eng. J.*, 2020, **383**, 123150.

73 P. K. Ray, R. Mohanty and K. Parida, Recent advancements of NiCo LDH and graphene based nanohybrids for supercapacitor application, *J. Energy Storage*, 2023, **72**, 108335.

74 Q. Bi, X. Hu and K. Tao, MOF-derived NiCo-LDH Nanocages on CuO Nanorod Arrays for Robust and High Energy Density Asymmetric Supercapacitors, *Chem. – Eur. J.*, 2023, **29**(11), e202203264.

75 L. Lei, X. Zhang, Y. Su, S. Wu and J. Shen, Metal–Organic Framework (MOF)-Assisted Construction of Core–Shell Nanoflower-like CuO/CF@NiCoMn–OH for High-Performance Supercapacitor, *Energy Fuels*, 2021, **35**(9), 8387–8395.

76 X. Deng, H. Qin, X. Liu, S. Zhu, J. Li, L. Ma and N. Zhao, Hierarchically porous trimetallic hydroxide arrays for aqueous energy storage and oxygen evolution with enhanced redox kinetics, *J. Alloys Compd.*, 2022, **918**, 165650.

77 Q. He, L. Han and K. Tao, Oxygen vacancy modulated Fe-doped Co3O4 hollow nanosheet arrays for efficient oxygen evolution reaction, *Chem. Commun.*, 2024, **60**(9), 1116–1119.

78 R. Kumar, S. Sahoo, E. Joanni, R. Pandey and J. J. Shim, Vacancy designed 2D materials for electrodes in energy storage devices, *Chem. Commun.*, 2023, **59**(41), 6109–6127.

79 M. U. Tahir, H. Arshad, H. Zhang, Z. Hou, J. Wang, C. Yang and X. Su, Room temperature and aqueous synthesis of bimetallic ZIF derived CoNi layered double hydroxides and their applications in asymmetric supercapacitors, *J. Colloid Interface Sci.*, 2020, **579**, 195–204.

80 Y. Li, B. Huang, X. Zhao, Z. Luo, S. Liang, H. Qin and L. Chen, Zeolitic imidazolate framework-L-assisted synthesis of inorganic and organic anion-intercalated hetero-trimetallic layered double hydroxide sheets as advanced electrode materials for aqueous asymmetric super-capacitor battery, *J. Power Sources*, 2022, **527**, 231149.

81 X. Zheng, Y. Sun, S. Jin, M. Xu, Y. Ding, F. Chen, T. Yang, Q. Zhang, X. Zheng and H. Chen, Sulfidation of ZIF-Derived Core-Shell NiCo LDH/Ni MOF Heterostructure toward Supercapacitor Electrodes with Enhanced Performance, *Batteries*, 2022, **8**(11), 241.

82 J. Tang, Y. Shen, X. Miao, H. Qin, D. Song, Y. Li, Y. Qu, Z. Yin, J. Ren, L. Wang and B. Wang, Template-directed growth of hierarchically structured MOF-derived LDH cage hybrid arrays for supercapacitor electrode, *J. Electroanal. Chem.*, 2019, **840**, 174–181.

83 Z. Xiao, Y. Bao, Z. Li, X. Huai, M. Wang, P. Liu and L. Wang, Construction of Hollow Cobalt–Nickel Phosphate Nanocages through a Controllable Etching Strategy for High Supercapacitor Performances, *ACS Appl. Energy Mater.*, 2019, **2**(2), 1086–1092.

84 Z. Yang, Q. Cheng, W. Li, Y. Li, C. Yang, K. Tao and L. Han, Construction of 2D ZIF-derived hierarchical and hollow NiCo-LDH "nanosheet-on-nanosheet" arrays on reduced graphene oxide/Ni foam for boosted electrochemical energy storage, *J. Aolloys Compd.*, 2021, **850**, 156864.

85 H. Jia, M. Wang, M. Feng, G. Li, L. Li and Y. Liu, Synergistic enhancement of supercapacitor performance: Modish designation of BPQD modified NiCo-LDH/NiCo2S4 hybrid nanotube arrays with improved conduc-

tivity and OH– adsorption, *Chem. Eng. J.*, 2024, **484**, 149591.
86 X. Wang, X. Song, J. Gao, Y. Zhang, K. Pan, H. Wang, L. Guo, P. Li, C. Huang and S. Yang, Effect of synthesis temperature on the structural morphology of a metal–organic framework and the capacitor performance of derived cobalt–nickel layered double hydroxides, *J. Colloid Interface Sci.*, 2024, **664**, 946–959.